



# The effect of rare-earth fission products on the rate of $U_3O_8$ formation on $UO_2$

R.J. McEachern<sup>\*</sup>, D.C. Doern, D.D. Wood

*Research Chemistry Branch, AECL, Whiteshell Laboratories, Pinawa, Man., Canada R0E 1L0*

Received 20 May 1997; accepted 22 August 1997

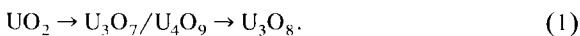
## Abstract

The rate of  $U_3O_8$  formation on the surface of flat neodymium-doped  $UO_2$  disks was measured by X-ray diffraction and the kinetic data were fitted to a two-dimensional nucleation-and-growth model. The results indicate that neodymium doping in the  $UO_2$  tends to inhibit  $U_3O_8$  formation. A quantitative relationship between the activation energy for  $U_3O_8$  formation and the neodymium content of the  $UO_2$  has been derived from the kinetic data. Our data are consistent with recent results obtained for the oxidation of used LWR fuel, which suggests that fission products in solid solution are likely the cause of  $U_3O_8$  inhibition observed for used fuel. © 1998 Elsevier Science B.V.

## 1. Introduction

In many countries, dry air storage is gaining acceptance for the intermediate storage of used nuclear fuel after several years of cooling under water and before final disposal in a geological repository [1]. One limitation of dry storage is the potential oxidation of fuel in the small number of elements that become defected in the reactor. In particular, the oxidation of  $UO_2$  to  $U_3O_8$  produces a 36% increase in volume of the fuel matrix, which can lead to splitting of the sheath and fuel spalling [2–4]. This can complicate subsequent handling and disposal of the fuel. Therefore, it is important to understand  $UO_2$  fuel oxidation in sufficient detail to define appropriate allowable conditions (such as time and temperature) for the safe handling and storage of used fuel.

It is widely known that  $UO_2$  oxidation proceeds by two stages [5–8]:



The formation of  $U_3O_7/U_4O_9$ <sup>1</sup> displays parabolic kinetic behaviour because this first stage of oxidation is controlled by the rate of oxygen diffusion through a discrete layer of the oxide product [11,12]. In contrast, the formation of  $U_3O_8$  displays sigmoidal reaction kinetics [2,13,14] consistent with a nucleation-and-growth mechanism [15].

The effect of dopants on the  $UO_2$  oxidation process has been studied for many years [16–21] because of the development of mixed-oxide and burnable-poison fuels in the nuclear industry and because dopants can influence the  $UO_2$  sintering process. Moreover, significant amounts of fission products are present as a solid solution in used fuel [22]. In particular, the effect of rare-earth (RE) dopants on the oxidation of  $UO_2$  has been studied extensively [18,23,24] because the RE are major fission products and

<sup>1</sup> The nature of the product of the first stage of  $UO_2$  oxidation varies depending on the oxidation conditions and the type of fuel. At low temperatures, spent light-water reactor (LWR) fuel, or  $UO_2$  with high dopant levels oxidizes to a cubic  $U_4O_{9+y}$  phase, whereas unirradiated  $UO_2$  oxidizes to tetragonal  $U_3O_7$  (see Refs. [9,10]). For simplicity, we use the unqualified terms  $U_3O_7/U_4O_9$  or  $U_3O_7$  to refer to the product of the first stage of  $UO_2$  oxidation.

<sup>\*</sup> Corresponding author. Present address: Chalk River Laboratories, AECL, Chalk River, Ont., Canada K0J 1J0. Tel.: +1-613 584 3311; fax: +1-613 584 1220; e-mail: mceacher@aecl.ca.

because of their use as burnable poisons [25]. Wilson et al. [18] noted increasing resistance to oxidation with increasing amounts of  $M_2O_3$  ( $M = Y, La$ ) in solid solution with  $UO_2$  when oxidized in air in the range 1375 to 1750°C. Thomas et al. [10] compared the oxidation at lower temperatures ( $< 600^\circ C$ ) of pure  $UO_2$  with doped materials containing 4 and 8 wt%  $Gd_2O_3$  as well as 0.4 wt%  $NbO_2$ , using thermal analysis and X-ray diffraction (XRD). They found that with each type of material the eventual product of oxidation was  $U_3O_8$  but that increasing dopant levels raised the threshold for  $U_3O_8$  formation in terms of both temperature and weight gain. Oxidation experiments performed on doped  $UO_2$  show that it commonly retains the fluorite-type structure to higher temperatures and for longer times, than the undoped material [10,17,21].

Considerable evidence suggests that used fuel displays oxidation resistance, similar to that shown by doped  $UO_2$ . It has been reported that the induction time ( $t_i$ ) for  $U_3O_8$  powder formation shows a positive correlation with burnup [26,27] although there is considerable scatter in the data. Similarly, Gilbert et al. [28] reported that unirradiated  $UO_2$ , or used fuel with a burnup below 15 MWd/kg U, oxidizes to  $U_3O_8$  more readily than used fuel with a burnup greater than 15 MWd/kg U. Choi et al. [29] studied the oxidation behaviour of simulated high-burnup nuclear fuel, i.e. SIMFUEL [30], and reported that the resistance to  $U_3O_8$  formation increased with burnup. There is not, however, unanimous agreement that burnup (or doping) is associated with increased oxidative resistance. Bennett et al. [31,32] oxidized advanced gas-cooled reactor (AGR) used-fuel fragments in air and found that  $t_i$  is somewhat shorter for used fuel than unirradiated  $UO_2$ . They also reported that there is no relationship between  $t_i$  and the extent of burnup in the range 11.7 to 26.7 MWd/kg U. It is difficult to rationalize the difference between oxidation behaviour reported by Bennett et al. [31,32] and others [26–29]; the differences are perhaps due to fuel microstructure.

The enhanced stability (relative to pure  $UO_2$ ) of the fluorite-type phase in doped  $UO_2$  or used fuel is thus generally well established, although there is not universal agreement on this point. However, the relationship between RE content and oxidation resistance has not yet been examined quantitatively. We have thus measured the kinetics of  $U_3O_8$  formation for a series of  $UO_2$  samples with a range of neodymium contents. The results are compared with data obtained with used fuel, and applications to the safe dry air storage of used nuclear fuel are discussed.

## 2. Experimental

### 2.1. Sample preparation and oxidation

Sintered pellets (12 mm diameter) of  $(U_{1-x}Nd_x)O_2$  ( $x = 0.01, 0.02$  or  $0.03$ ) were prepared by mixing finely

divided  $Nd_2O_3$  and  $UO_2$  powders, cold pressing, and then sintering in a hydrogen (10%)/nitrogen atmosphere at 1650°C for 2 h. The homogeneity of this material was confirmed by scanning electron microscopy/energy dispersive X-ray spectroscopy. The oxidation behaviour of neodymium-doped  $UO_2$  was compared with that of undoped CANDU<sup>®</sup> 2 fuel pellets.

For each sample, disks about 2 mm thick were cut from the cylindrical pellet using a low-speed diamond saw. One surface of each disk was then polished manually using 400-grit abrasive paper. Previous work with  $UO_2$  has shown that the rate of formation of  $U_3O_8$  is more reproducible on a surface with a 400-grit finish than on more highly polished surfaces, where  $U_3O_8$  nucleates preferentially at cracks and other flaws [33]. After polishing, the disks were cleaned with ethanol and then distilled water prior to oxidation. The samples were then oxidized in unlimited laboratory air in a convection oven with temperature control accurate to within 2°C. At selected intervals, each sample was cooled to room temperature and the XRD pattern was recorded. Samples were then returned to the oven, and the heat treatment (at the same temperature) was continued. The heat-cool-analyze cycle was continued until there was visible evidence of  $U_3O_8$  powder formation on the sample surface. At such time, the experiments were terminated, because powder formation and spalling negate the XRD data. Surface oxidation of doped  $UO_2$  samples generally only proceeded to 10–20% before the samples crumbled. Air-oxidation experiments were performed at 200, 225, 250, 260, 275, 300 and 325°C. Oxidation times varied with temperature and were in the range 1 to 5000 h.

### 2.2. Collection and quantitative treatment of the XRD data

The XRD data were collected using a Rigaku Rotaflex diffractometer equipped with a 12 kW rotating-anode Cu K $\alpha$  source and a diffracted-beam monochromator. The diffractometer scanning rate was 10° ( $2\theta$ )/min for qualitative peak identification and 1° ( $2\theta$ )/min for the acquisition of integrated intensities for specific peaks.

The progress of  $U_3O_8$  formation was followed by monitoring XRD peak intensities, using the procedure developed by Choi et al. [29]. Thus the fraction of the surface oxidized to  $U_3O_8$  was determined for each sample by measuring the integrated intensity of the overlapping [200] and [130] peaks for  $U_3O_8$  ( $2\theta \approx 26.0^\circ$  with Cu K $\alpha$  radiation) and the [111] feature for  $U_3O_7/U_4O_9$  ( $2\theta \approx 28.5^\circ$ ). These intensities were termed  $I_{U_3O_8}$  and  $I_{U_3O_7}$ , respectively. From these intensities, the fraction,  $F$ , of the surface oxidized to  $U_3O_8$  will be given by [29]

$$F = \frac{I_{U_3O_8}}{I_{U_3O_8} + \alpha I_{U_3O_7}}, \quad (2)$$

<sup>®</sup> CANDU<sup>®</sup> is a registered trademark of Atomic Energy of Canada.

where the empirical factor ( $\alpha$ ) accounts for the different absolute XRD intensities and mass absorption coefficients of  $U_3O_8$  and  $U_3O_7$ . Previously published results have shown that  $\alpha$  is  $0.450 \pm 0.033$  [29].

The XRD analysis depth in our samples is approximately  $1 \mu\text{m}$  for the selected XRD peaks [9,29]. The formation of  $U_3O_8$  on the surface of the 12 mm disks can thus be considered equivalent to a two-dimensional nucleation-and-growth reaction mechanism. Recently, McEachern et al. [34] showed that such two-dimensional reaction kinetics can be modelled by

$$F(t) = 1 - \exp\left\{-\frac{\pi\kappa t^3}{3} + \frac{\pi^2\kappa^2 t^6}{180} - \frac{11\pi^3\kappa^3 t^9}{45360} + \frac{5\pi^4\kappa^4 t^{12}}{399168}\right\} \quad (3)$$

where  $F$  is the fraction of the surface oxidized,  $t$  is the time and  $\kappa$  is an effective rate constant, defined by

$$\kappa = K_g^2 K_n, \quad (4)$$

where  $K_n$  ( $\text{s}^{-1} \text{m}^{-2}$ ) is the rate of nucleation per unit area and  $K_g$  ( $\text{m s}^{-1}$ ) is the rate of linear growth of the circular nuclei.

### 3. Results and discussion

For each sample,  $I_{U_3O_8}$  and  $I_{U_3O_7}$  were measured from the XRD data and the fraction of the sample surface converted to  $U_3O_8$  was calculated by use of Eq. (2). Each experimental run yielded a series of  $F$  values obtained at various times during the course of the reaction. The value of the rate constant,  $\kappa$ , was then calculated for each temperature and dopant concentration by minimizing the sum of the squares of deviations between calculated and experimental values of  $F$  according to Eq. (3). The results are displayed in Table 1. Typical agreement between the experimental data and the curves obtained by fitting these data to Eq. (3) is displayed in Fig. 1.

An Arrhenius plot for the composite rate constant  $\kappa$  is

Table 1  
Experimental values of the composite rate constant,  $\kappa$  ( $\text{h}^{-3}$ ) for various temperatures and neodymium concentrations

Temperature (°C)	Neodymium concentration (at.%)			
	0.0	1.0	2.0	3.0
200	$2.1 \times 10^{-12}$	$2.0 \times 10^{-13}$	$4.9 \times 10^{-14}$	$7.3 \times 10^{-14}$
225	$4.1 \times 10^{-10}$	$4.3 \times 10^{-11}$	$1.1 \times 10^{-11}$	$1.5 \times 10^{-11}$
250	$8.2 \times 10^{-7}$	$8.8 \times 10^{-7}$	$5.8 \times 10^{-7}$	$2.9 \times 10^{-7}$
260	$8.3 \times 10^{-7}$	$2.3 \times 10^{-7}$	$4.4 \times 10^{-8}$	$3.5 \times 10^{-8}$
275	$9.2 \times 10^{-5}$	$7.0 \times 10^{-5}$	$2.8 \times 10^{-5}$	$2.6 \times 10^{-5}$
300	$2.0 \times 10^{-3}$	$5.5 \times 10^{-4}$	$3.7 \times 10^{-4}$	$3.2 \times 10^{-4}$
325	$6.1 \times 10^{-3}$	$4.4 \times 10^{-3}$	$1.3 \times 10^{-3}$	$7.7 \times 10^{-4}$

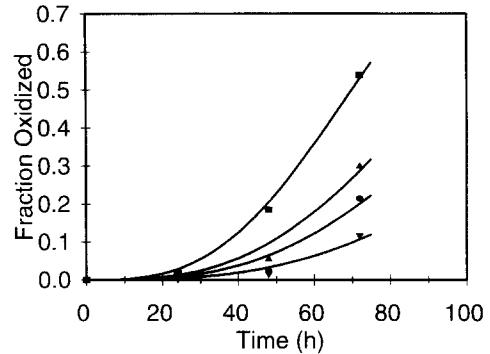


Fig. 1. Fraction of the sample surface oxidized to  $U_3O_8$  for  $UO_2$  disks doped with 0.0 (■), 1.0 (▲), 2.0 (●) or 3.0 (▼) at.% neodymium when heated at  $250^\circ\text{C}$  in air.

displayed in Fig. 2. Data for  $325^\circ\text{C}$  are not included in Fig. 2 because they deviate from linearity; other workers have reported similar observations above  $300^\circ\text{C}$  [2,35–37]. The reasons for such non-linearity are not well known. It may be due to experimental difficulties associated with the relatively short reaction times, or to a change in oxidation mechanism around  $300$  to  $350^\circ\text{C}$  [2,35–37]. The Arrhenius expression was calculated (200 to  $300^\circ\text{C}$ ) for each neodymium concentration shown in Fig. 2. The results were as follows<sup>3</sup>:

$$0 \text{ at.}\% \ln(\kappa) = -\frac{5.81 \times 10^4}{T(\text{K})} + 95.88, \quad (5)$$

$$1 \text{ at.}\% \ln(\kappa) = -\frac{6.32 \times 10^4}{T(\text{K})} + 104.66, \quad (6)$$

$$2 \text{ at.}\% \ln(\kappa) = -\frac{6.54 \times 10^4}{T(\text{K})} + 107.70, \quad (7)$$

$$3 \text{ at.}\% \ln(\kappa) = -\frac{6.40 \times 10^4}{T(\text{K})} + 105.04. \quad (8)$$

The activation energy was calculated for each of the Arrhenius expressions (Eqs. (5)–(8)) which exclude the  $325^\circ\text{C}$  data. The result obtained for each neodymium composition is given in Table 2 and a plot of the activation energy as a function of neodymium concentration is given in Fig. 3. The uncertainty in the reported activation energies is taken to be  $10 \text{ kJ mol}^{-1}$  (90% confidence interval) based on a similar analysis reported earlier [34]. The data in Fig. 3 can be fitted approximately to a linear relationship between the activation energy for  $U_3O_8$  formation and neodymium content of the doped  $UO_2$ :

$$E_{\text{act}} = 166 \text{ kJ mol}^{-1} + 5.46x, \quad (9)$$

<sup>3</sup> Throughout this report the term at.% refers to the fraction of the total metal content on an oxygen-free basis.

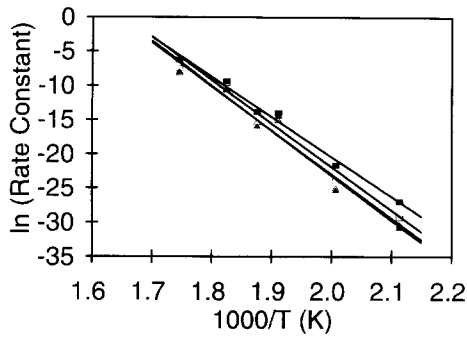


Fig. 2. Arrhenius plot for the composite rate constant  $\kappa$  for  $U_3O_8$  formation for  $UO_2$  doped with 0.0 (■), 1.0 (□), 2.0 (▲) or 3.0 (△) at.% neodymium.

where  $x$  is the neodymium concentration of the  $(U, Nd)O_2$  in at.%. The dependence of  $E_{act}$  on  $x$  is not statistically significant at the 95% confidence level. The effect of neodymium on the *rate* of oxidation, however, is genuine (Table 1).

Direct comparison between our data and that obtained for used fuel is difficult because the composition and structure of used fuel are quite variable. However, a rough comparison between used-fuel data and our results is instructive. Gilbert et al. [26] found a positive correlation between burnup and the (normalized) powder induction time. Examination of their Fig. 1 reveals that the time required for  $U_3O_8$  powder formation around 250°C is an order of magnitude greater for used fuel with a burnup of 25 to 30 MWd/kg U ( $\sim 2.9$  at.%)<sup>4</sup> than for pure  $UO_2$ . Similarly, Choi et al. [29] found that the time required for  $U_3O_8$  powder formation at 250°C is an order of magnitude longer for SIMFUEL with a simulated burnup of  $\sim 4.9$  at.% than for pure  $UO_2$  (based on eq. 11 of Ref. [29]).

Based on the results obtained by Gilbert et al. [26] and Choi et al. [29], we conclude that the rate of  $U_3O_8$  formation on unirradiated  $UO_2$  will be an order of magnitude faster than for used fuel with a burnup between 2.9 and 4.9 at.%. Taking the average of these two results, we assume that (to a first approximation) the rate of oxidation for  $UO_2$  will be an order of magnitude faster than for used fuel with a burnup of  $\sim 3.9$  at.%. The rare-earth content of used fuel with a burnup of 3.9 at.% is  $\sim 1.8$  at.% [22]. To compare the data for used fuel and SIMFUEL with our results, one can calculate from Eqs. (5) and (7) that at 250°C the rate constant,  $\kappa$  is  $2.28 \times 10^{-7} h^{-3}$  for  $UO_2$  and  $2.42 \times 10^{-8} h^{-3}$  for  $UO_2$  doped with 2.0 at.% Nd. Using these values of  $\kappa$  one can estimate (Eq. (3)) that oxidation for 100 h at 250°C will result in  $F$  values of 0.212 for  $UO_2$  and 0.025 for  $UO_2$  doped with 2.0 at.% Nd. Thus the same 'order-of-magnitude' decrease in reactivity

Table 2

Activation energy for the formation of  $U_3O_8$  on the surface of  $UO_2$  disks doped with various concentrations of neodymium

Neodymium concentration (at.%)	$E_{act}$ (kJ mol <sup>-1</sup> )
0.0	161.1
1.0	175.3
2.0	181.3
3.0	177.3

is observed for  $UO_2$  doped with 2 at.% neodymium as for used fuel with a fission-product rare-earth content of  $\sim 1.8$  at.%. Our analysis is clearly only approximate, but it seems reasonable to conclude that used fuel is less prone to air oxidation than unirradiated  $UO_2$  because of rare-earth (and other) fission products present in solid solution in the used fuel.

The lower rate of oxidation for rare-earth doped  $UO_2$  relative to that of the pure material is consistent with results obtained by Thomas et al. [10] for  $UO_2$  doped with gadolinium or with niobium. Our data are also consistent with results reported by Choi et al. [29], who examined the air oxidation of SIMFUEL. Neither SIMFUEL nor rare-earth-doped  $UO_2$  replicate the fission-gas bubble formation and other microstructural details of used fuels. Thus our results do not support the suggestion of Gilbert et al. [28] that increased oxygen grain boundary diffusion rates in used fuel may be responsible for the observed slower rate of  $U_3O_8$  formation in this material than in  $UO_2$ .

#### 4. Conclusions

X-ray powder diffraction was used to quantify the rate of  $U_3O_8$  formation on the surface of neodymium-doped  $UO_2$  disks oxidized in air. The kinetic data were fitted to a two-dimensional nucleation-and-growth model, published earlier, and the results were used to develop a quantitative relationship between the  $U_3O_8$ -formation rate constant,  $\kappa$ , and the neodymium content of the  $(U, Nd)O_2$ .

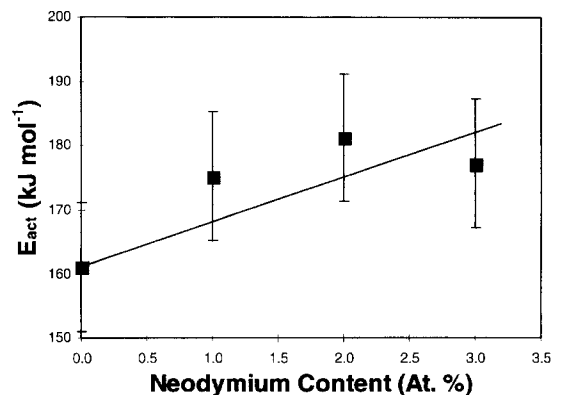


Fig. 3. Activation energy for the formation of  $U_3O_8$  on the surface of  $UO_2$  disks doped with various amounts of neodymium.

<sup>4</sup> 1 at.% burnup is equivalent to  $\sim 9.46$  MWd/kg U.

Our data show that increased neodymium content of doped  $\text{UO}_2$  results in longer  $\text{U}_3\text{O}_8$  powder-formation times, which is consistent with results obtained for used LWR fuel and SIMFUEL. It thus appears that high-burnup used fuel is more resistant to  $\text{U}_3\text{O}_8$  formation than low-burnup used fuel, and that this is due, at least in part, to rare-earth (and other) fission products present in solid solution in the used fuel.

Our results indicate that unirradiated  $\text{UO}_2$  data can be used judiciously for conservative calculations of rates of  $\text{U}_3\text{O}_8$  formation on used fuels under dry storage conditions.

### Acknowledgements

The authors appreciate critical review of the manuscript by J. McFarlane and P. Taylor. We also would like to thank H. Hamilton and J. Sullivan (Fuel Materials Branch, Chalk River Laboratories) for fabrication of the neodymium-doped  $\text{UO}_2$  pellets.

### References

- [1] K.J. Schneider, S.J. Mitchell, A.B. Johnson, Jr. in: Proc. 3rd Int. Conf. on High Level Radioactive Waste Management, Las Vegas, NV, Apr. 13–17, American Nuclear Society, La Grange Park, IL and American Society of Civil Engineers, New York, NY, 1992, p. 1159.
- [2] D.G. Boase, T.T. Vandergraaf, Nucl. Technol. 32 (1977) 60.
- [3] J. Novak, I.J. Hastings, E. Mizzan, R.J. Chenier, Nucl. Technol. 63 (1983) 254.
- [4] R.E. Einziger, J.A. Cook, Nucl. Technol. 69 (1985) 55.
- [5] P.E. Blackburn, J. Weissbart, E.A. Gulbransen, J. Phys. Chem. 62 (1958) 902.
- [6] J. Belle (Ed.), Uranium dioxide: Properties and Nuclear Applications, Naval Reactors, Division of Reactor Development, USAEC, 1961.
- [7] H. Ohashi, H. Hayashi, M. Nabeshima, T. Morozumi, Bull. Fac. Eng. Hokkaido Univ. 134 (1987) 49.
- [8] R.J. McEachern, P. Taylor, A review of the oxidation of uranium dioxide at temperatures below 400°C, Atomic Energy of Canada, Report AECL-11335, COG-95-281-I.
- [9] P. Taylor, E.A. Burgess, D.G. Owen, J. Nucl. Mater. 88 (1980) 153.
- [10] L.E. Thomas, R.E. Einziger, H.C. Buchanan, J. Nucl. Mater. 201 (1993) 310.
- [11] H.R. Hoekstra, A. Santoro, S. Siegel, J. Inorg. Nucl. Chem. 18 (1961) 166.
- [12] L.E. Thomas, R.E. Einziger, Mater. Charact. 28 (1992) 149.
- [13] K.T. Harrison, C. Padgett, K.T. Scott, J. Nucl. Mater. 23 (1967) 121.
- [14] J. Nakamura, T. Otomo, S. Kawasaki, J. Nucl. Sci. Technol. 30 (1993) 181.
- [15] S. Aronson, R.B. Roof Jr., J. Belle, J. Chem. Phys. 27 (1957) 137.
- [16] J.S. Anderson, K.D.B. Johnson, J. Chem. Soc. (1953) 1731.
- [17] J.S. Anderson, D.N. Edgington, L.E.J. Roberts, E. Wait, J. Chem. Soc. London 3 (1954) 3324.
- [18] W.B. Wilson, C.A. Alexander, A.F. Gerds, J. Inorg. Nucl. Chem. 20 (1961) 242.
- [19] D.C. Hill, J. Am. Ceram. Soc. 45 (1962) 258.
- [20] S.F. Bartram, E.F. Juenke, E.A. Aitken, J. Am. Ceram. Soc. 47 (1964) 171.
- [21] V.J. Tennery, T.G. Godfrey, J. Am. Ceram. Soc. 56 (1973) 129.
- [22] R.J. Guenther, D.E. Blahnik, T.K. Campbell, U.P. Jenquin, J.E. Mendel, C.K. Thornhill, Characterization of spent fuel approved testing material ATM-106, Pacific Northwest Laboratory Report PNL-5109-106, UC-70, 1988.
- [23] L.E.J. Roberts, L.E. Russell, A.G. Adwick, A.J. Walter, M.H. Rand, in: Proc. of UN Conf. on the Peaceful Uses of Atomic Energy, 1959, p. 215.
- [24] C.R.A. Catlow, J. Nucl. Mater. 79 (1979) 432.
- [25] H. Bairiot, P. Deramaix, C. Vandenberg, Belgian contributions to improved fuel utilization, in: Improved Utilization of Water Reactor Fuel, with Special Emphasis on Extended Burnups and Plutonium Recycling, Proc. of the Special Meeting, IAEA Report CONF-8405285, 1984, pp. 86–97.
- [26] E.R. Gilbert, C.A. Knox, G.D. White, A.B. Johnson Jr., Am. Nucl. Soc. Trans. 50 (1985) 117.
- [27] D.J. Wheeler, Proc. Workshop on Chemical Reactivity of Oxide Fuel and Fission Product Release, Berkeley Nuclear Laboratories, UK, Apr. 7–9, Central Electricity Generating Board, UK, Technology Planning and Research Division, 1987.
- [28] E.R. Gilbert, G.D. White, C.A. Knox, Proc. Int. Workshop on Irradiated Fuel Storage: Operating Experience and Development Programs, Toronto, ON, Canada, Oct. 17–18, 1984.
- [29] J.W. Choi, R.J. McEachern, P. Taylor, D.D. Wood, J. Nucl. Mater. 230 (1996) 250.
- [30] P.G. Lucuta, R.A. Verrall, H.J. Matzke, B.J. Palmer, J. Nucl. Mater. 178 (1991) 48.
- [31] P. Wood, M.J. Bennett, M.R. Houlton, J.B. Price, Proc. British Nuclear Energy Society Conference on Nuclear Fuel Performance, Stratford-upon-Avon, UK, Mar. 25–29, British Nuclear Energy Society, UK, 1985.
- [32] M.J. Bennett, J.B. Price, P. Wood, Nucl. Energy 27 (1988) 49.
- [33] P. Taylor, D.D. Wood, A.M. Duclos, J. Nucl. Mater. 189 (1992) 116.
- [34] R.J. McEachern, J.W. Choi, M. Kolar, W. Long, P. Taylor, D.D. Wood, J. Nucl. Mater. 249 (1997) 58.
- [35] P.M. Tucker, in: K.A. Simpson, P. Wood (Eds.), Proc. Workshop on Chemical Reactivity on Oxide Fuel and Fission Product Release, Berkeley, UK, CEGB, London, 1987, p. 49.
- [36] K.A. Simpson, P. Wood, Proc. Nuclear Regulatory Commission Workshop on Spent Fuel/Cladding Reactions During Dry Storage, Gaithersburg, MD, Aug. 17–18, Nuclear Regulatory Commission, 1983; Also Nuclear Regulatory Commission Report NUREG/CP-0049.
- [37] P. Wood, G.G. Bannister, in: K.A. Simpson, P. Wood (Eds.), Proc. Workshop on Chemical Reactivity on Oxide Fuel and Fission Product Release, Berkeley, UK, CEGB, London, 1987, p. 19.